Electronic Supplementary Information

In-situ carbon encapsulation of vertical MoS_2 arrays with SnO_2 for durable high rate lithium storage: dominated pseudocapacitive

Mengjiao Li, *Qinglin Deng*, *Junyong Wang*, *Kai Jiang*, *Zhigao Hu* [a], and *Junhao Chu*

Key Laboratory of Polar Materials and Devices (MOE) and Technical Center for Multifunctional Magneto-Optical Spectroscopy (Shanghai), Department of Electronic Engineering, East China Normal University, Shanghai 200241, China

[a] Author to whom correspondence should be addressed.

Tel.: +86-21-54345150. Fax: +86-21-54345119.

Electronic mail: zghu@ee.ecnu.edu.cn

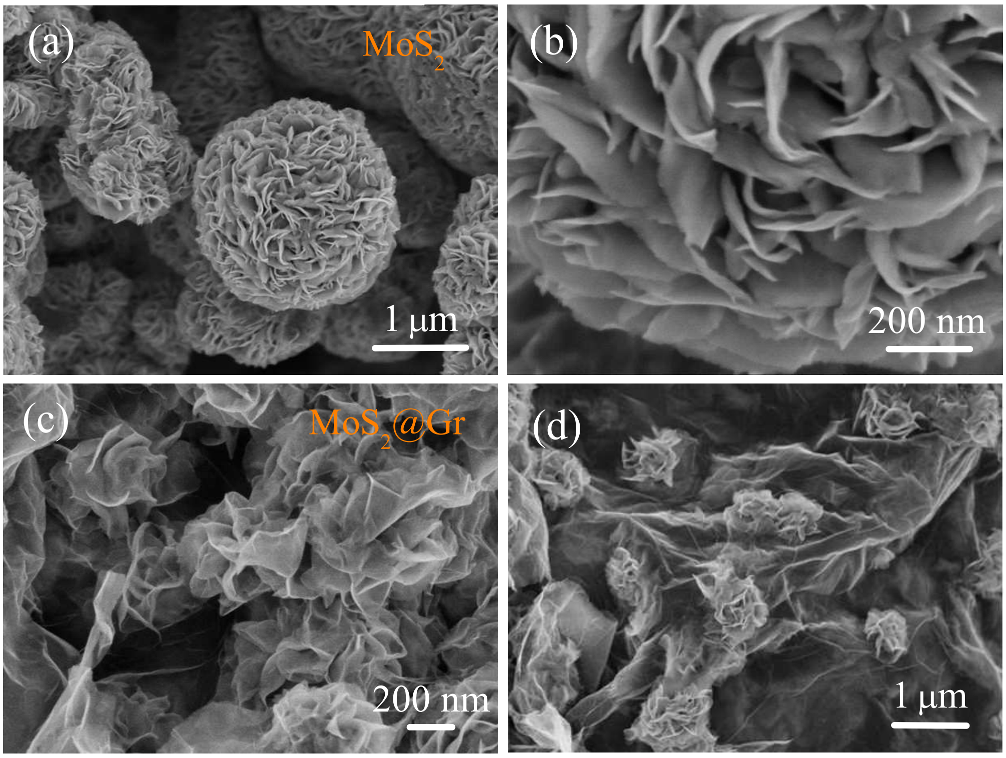

Figure 1: SEM images of (a)-(b) pure MoS_2 and (c)-(d) MoS_2@Gr composites at different magnifications.

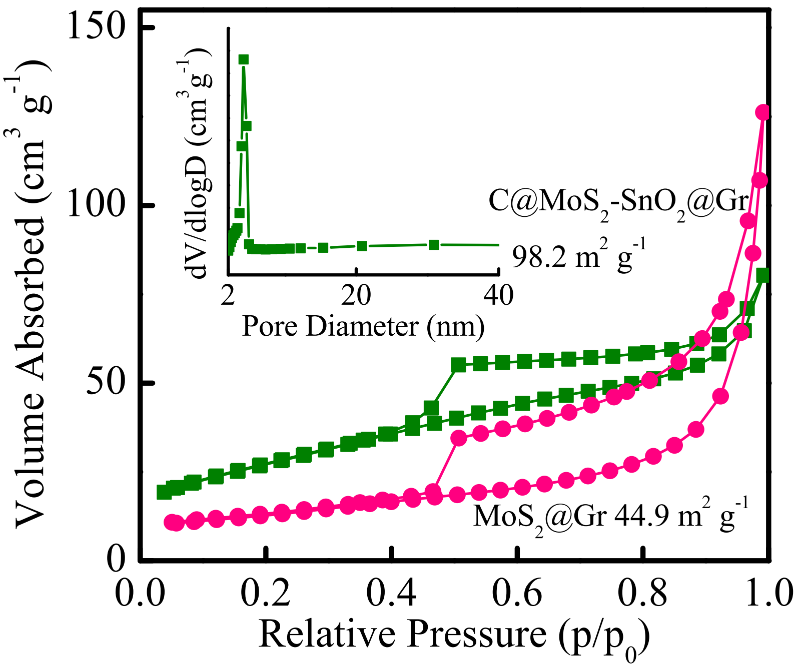

Figure 2: Nitrogen adsorption-desorption isotherms and the pore-size distribution (inset) of C@MoS_2-SnO_2@Gr and MoS_2.

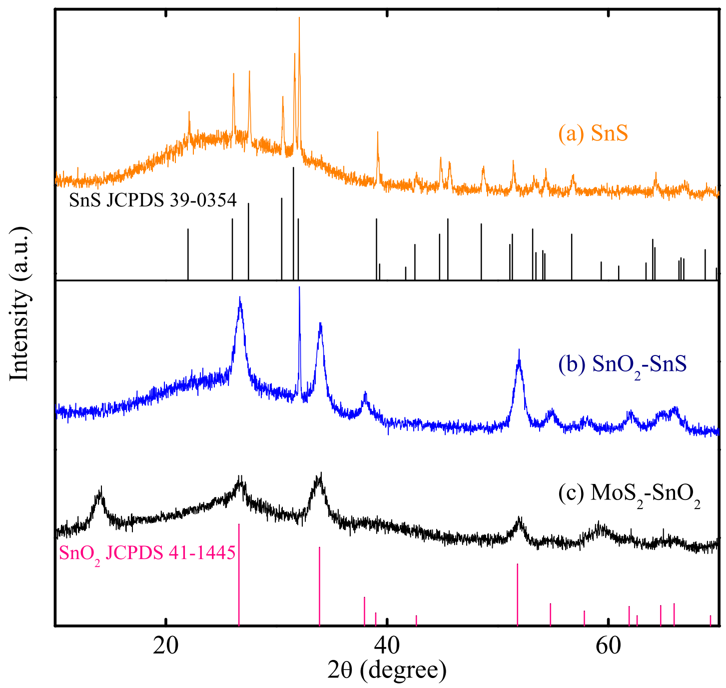

Figure 3: The XRD pattern of (a) SnS (JCPDS 39-0354) obtained from H_2SnO_3 precursor and thioacetamide; (b) SnO_2-SnS collected from H_2SnO_3 precursor and thiourea; (c) MoS_2-SnO_2 obtained from $Na_2MoO_4{\cdot}2H_2O$, H_2SnO_3 precursor, and thiourea.

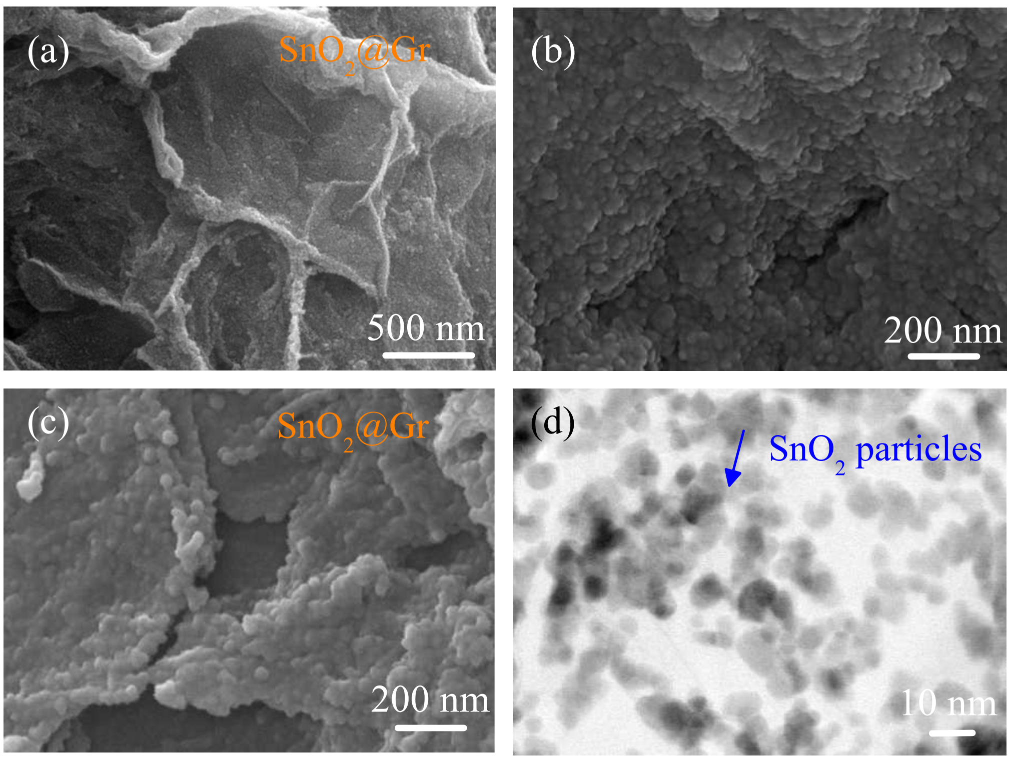

Figure 4: (a)-(c) SEM images and (d) TEM images of SnO_2@Gr at different magnifications. Note that the size of the SnO_2 nanoparticles reach about 5-8 nm.

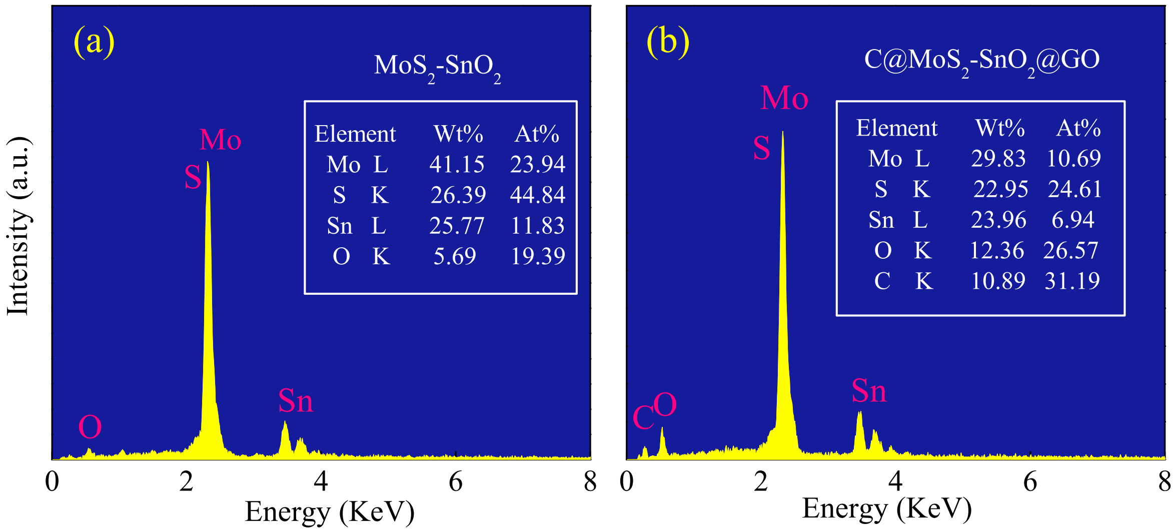

Figure 5: EDS spectra of (a) MoS_2-SnO_2 and (b) C@MoS_2-SnO_2@Gr samples, respectively.

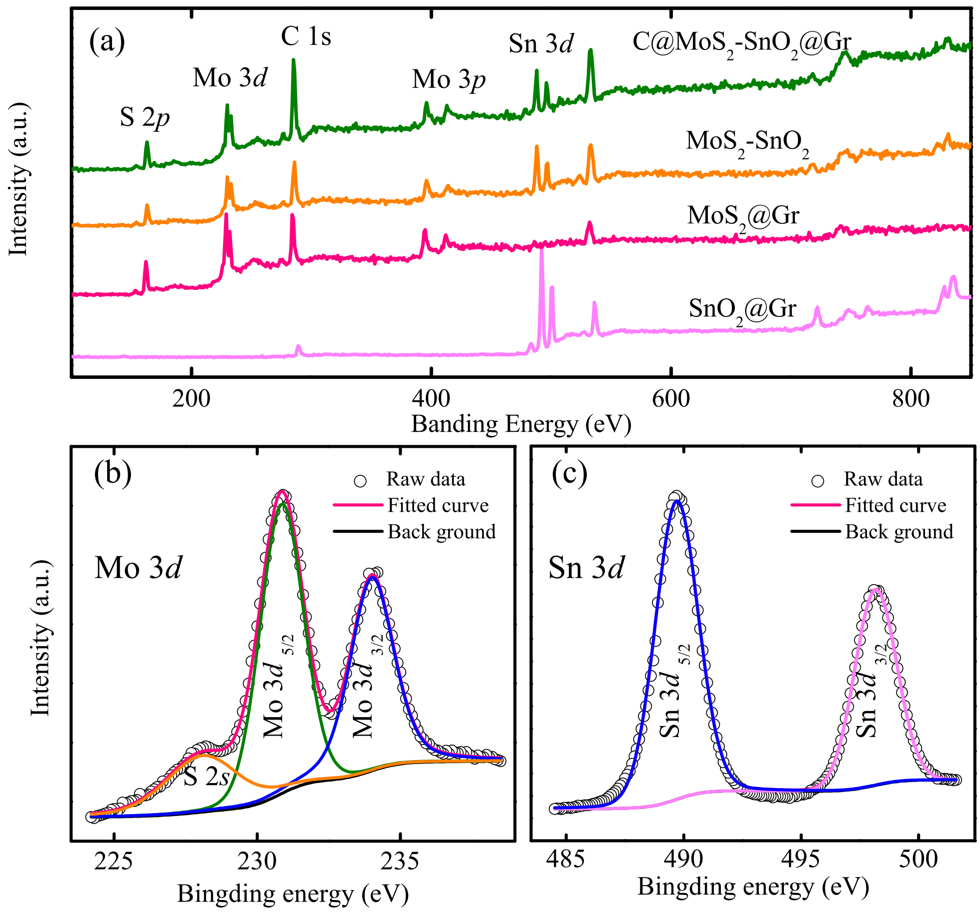

Figure 6: (a) The XPS survey spectra of as-fabricated samples. The high-resolution and fitted resulted of (b) Mo 3d and (c) Sn 3d of MoS_2@Gr and SnO_2@Gr hybrids, respectively.

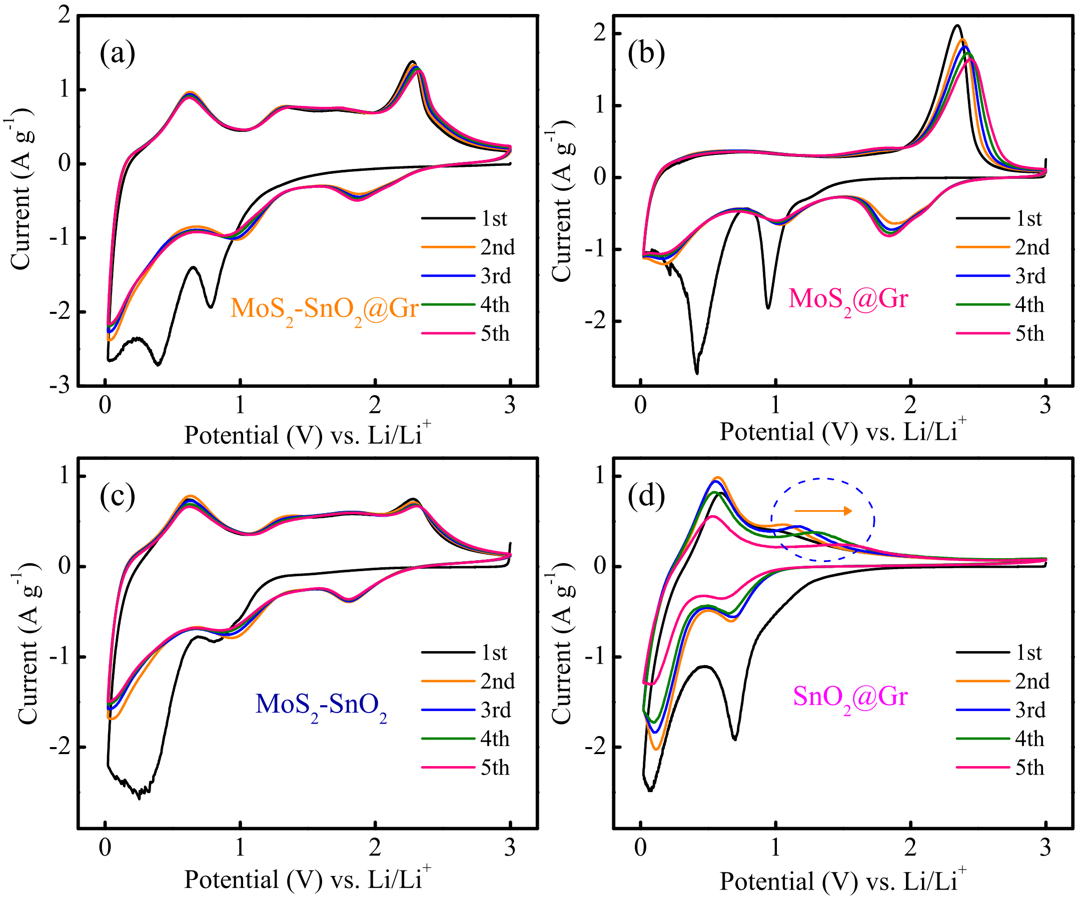

Figure 7: (a)-(d) Cyclic voltammograms (CV) curves for the first five cycles of MoS_2-SnO_2@Gr, MoS_2@Gr, MoS_2-SnO_2, and SnO_2@Gr, respectively.

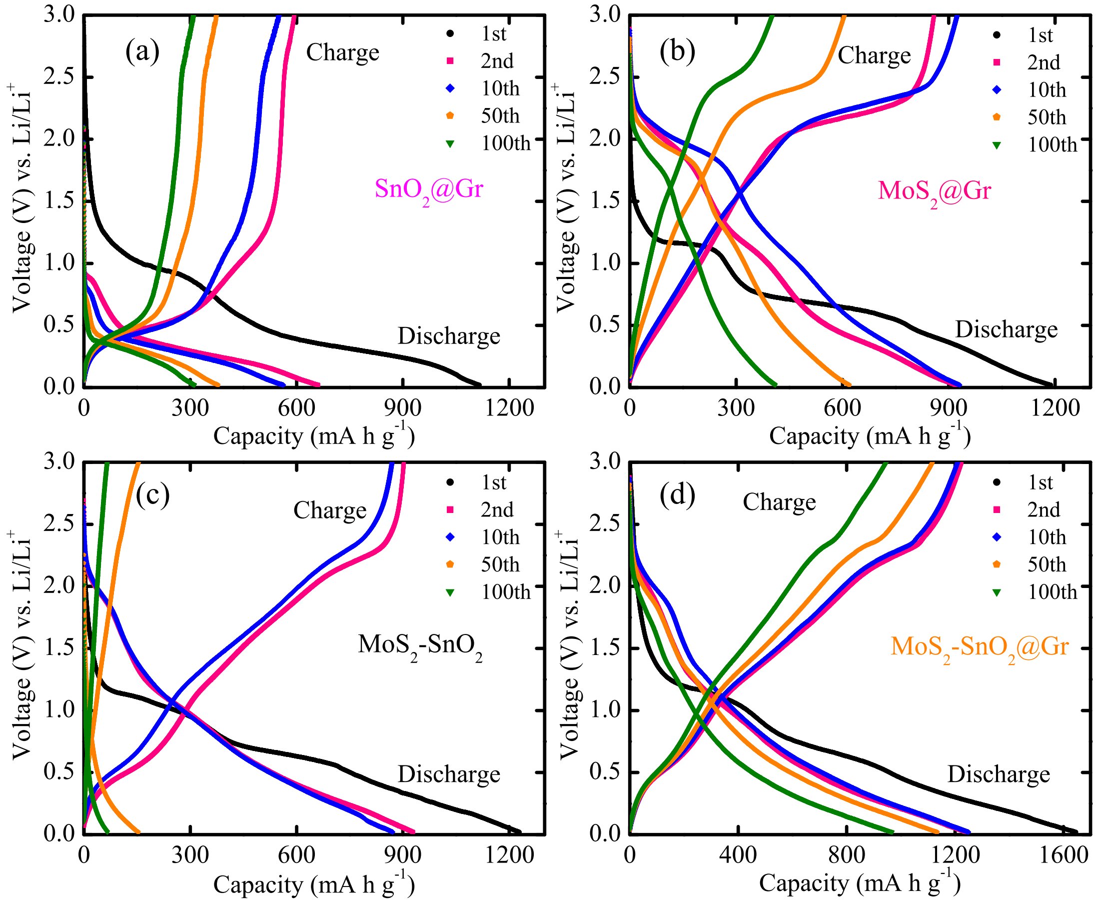

Figure 8: (a)-(d) The galvanostatic discharge-charge (GDC) profiles of SnO_2@Gr, MoS_2@Gr, MoS_2-SnO_2, and MoS_2-SnO_2@Gr for 1st, 2nd, 10th, 50th, and 100th cycles at 0.1 A g^{-1}.

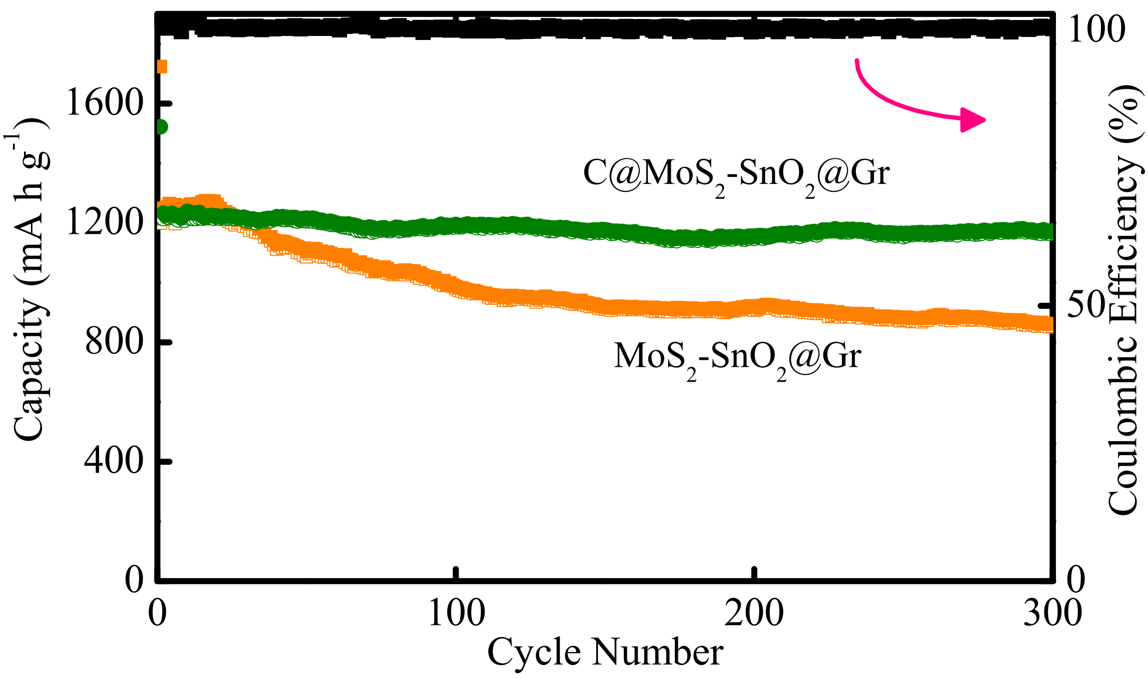

Figure 9: (a)-(d) The cycling stability of the C@MoS_2-SnO_2@Gr and MoS_2-SnO_2@Gr electrodes at 0.1 A g^{-1} for 300 cycles.

Table 1: Recent works of MoS_2/SnO_2 graphene-based anode materials for LIBs

Anode materials	discharge current density (mA g^{-1})	cycle	capacity (mA h g^{-1})	capacity retention	Ref.
MoS_2@vertical-Gr	200	100th	1109	88%	1
MoS_2@Gr	1000	200th	740	84%	2
MoS_2@crumpled-Gr	500	250th	680	60%	3
Polypyrrole-SnO_2	200	200th	790	72%	4
Polyaniline-C-SnO_2@Gr	1000	100th	540	70%	5
C-Sn-MoS_2-SnO_2	200	100th	861	80%	6
C@MoS_2-SnO_2@Gr	100	300th	1170	95%	This work
C@MoS_2-SnO_2@Gr	800	200th	1070	90%	This work

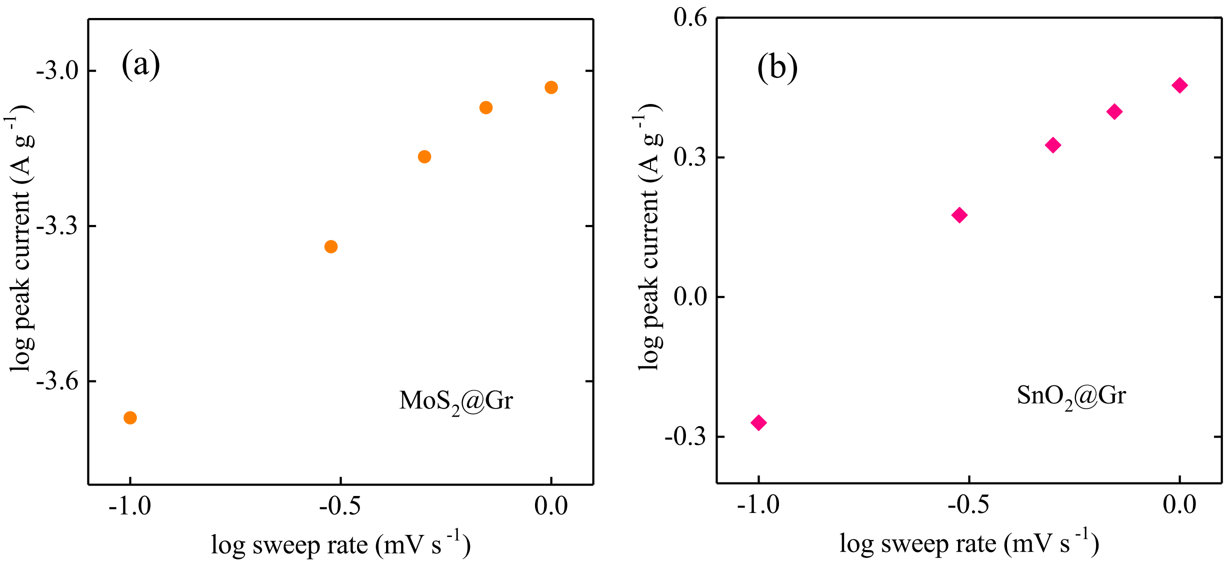

Figure 10: The specific peak currents at various sweep rates from 0.1-1 mV s^{-1} of (a) MoS_2@Gr and (b) SnO_2@Gr, respectively.

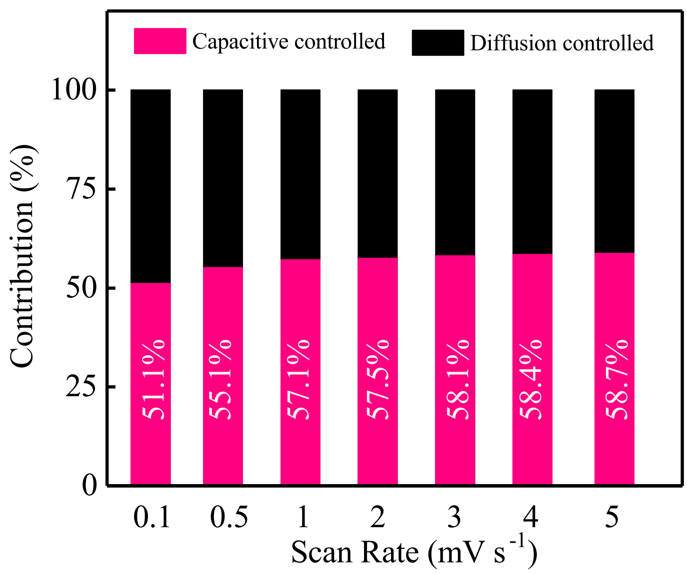

Figure 11: Normalized capacitive contribution ratio of MoS_2@Gr electrode at various rates.

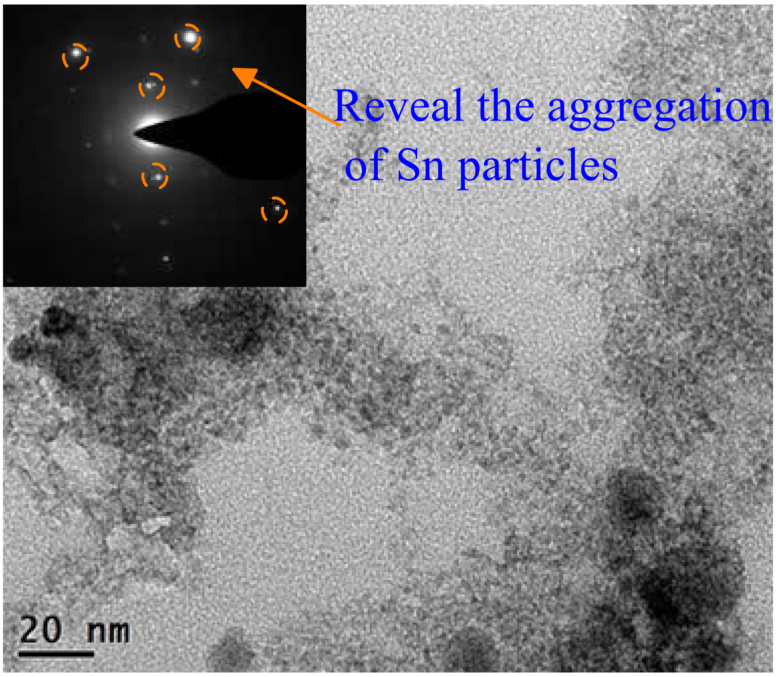

Figure 12: The TEM image of SnO_2@Gr electrode after GDC cycles. The inset is the SEAD pattern, which reveals the worse reversibility of SnO_2 and serious aggregation of Sn particles.

References

[1] Y. Wang, B. Chen, D. H. Seo, Z. J. Han, J. I. Wong, K. Ostrikov, H. Zhang. H. Y. Yang, *NPG Asia Materials*, **2016**, 8, e268.

[2] Y. Liu, X. Z. Wang, X. D. Song, Y. F. Dong, L. Yang, L. X. Wang, D. Z. Jia, Z. B. Zhao, J. S. Qiu, *Carbon*, **2016**, 109, 461-471.

[3] F. Y. Xiong, Z. Y. Cai, L. B. Qu, P. F. Zhang, Z. F. Yuan, O. K. Asare, W. W. Xu, C. Lin, L. Q. Mai, *ACS Appl. Mater. Interfaces*, **2015**, 7, 12625-12630.

[4] X. F. Du, T. J. Yang, J. Lin, T. Y. Feng, J. B. Zhu, L. Lu, Y. L. Xu, J. P. Wang, *ACS Appl. Mater. Interfaces*, **2016**, 8, 15598.

[5] F. Ye, B. T. Zhao, R. Ran, Z. P. Shao, *J. Power Sources*, **2015**, 290, 61-70.

[6] Y. G. Huang, Q. C. Pan, H. Q. Wang, C. Ji, X. M. Wu, Z. Q. He, Q. Y. Li, *J. Mater. Chem. A*, **2016**, 4, 7185.